The localised wrinkling of a stretched bi-annular thin plate

Xiang Liu, Ciprian Coman

Abstract—The wrinkling of a thin elastic bi-annular plate with piecewise-constant mechanical properties, subjected to radial stretching, is considered. The critical wrinkling stretching loading and the corresponding wrinkling patterns are extensively investigated, together with the roles played by both the geometrical and mechanical parameters.

Keywords—bi-annular plate, wrinkling pattern, critical stretching loading.

I. INTRODUCTION

WRINKLING of thin structures such as thin plates and shells is a common occurrence in solid mechanics. Largely speaking, the wrinkling is attributed to their lack of bending rigidity that makes them susceptible to buckle under compression. However, this does not preclude the occurrence of wrinkles in systems subjected to global tensile loads. Indeed, geometrical discontinuities in an elastic solid are known to redistribute the stresses applied on its boundary, thus leading to unexpected regions of compressive stresses inside the solid. An interesting example is the localised wrinkling of an annular plate near its inner rim when it is subjected to radial stretching along its boundaries, which have been explored both experimentally [10] and analytically [4], [5].

The motivation of the present work originates partly from the above localised wrinkling regime, and partly by the work of Simitses and Frostig [8], [9], [14]. In [8], the authors formulated the classical buckling problem of a multi-annular plate subjected to axisymmetric radial compressive loading on the boundaries or the common joints, which is followed by the numerical study of a uniformly compressed bi-annular plate using a power series method. Later, this strategy was expanded for a ring-stiffened annular plate under compression, to discuss the effect of boundary conditions and its rigidities on its buckling [9], [14]. In this paper, we discuss a stretched bi-annular plate with piecewise-constant mechanical properties. This bi-annular plate is composed of two fully bounded annuli, which are made of different materials with different Young's moduli and Poisson ratios. Comparing with the stretched single-annular plate by Coman *et al.* [4], [5], the discontinuities between the materials of the two annuli raise a couple of interesting questions:

A question with engineering practical concerns comes to us: how is the mechanical properties of each annuli attribute to the resistance of wrinkling? Since it is of practical importance for the design with respect to the buckling failure.

X. Liu is with the Department of Mathematics & Statistics, University of Glasgow, Scotland, UK e-mail: x.liu@maths.gla.ac.uk

C. Coman is with University of Glasgow

The question that follows is, the work in [5] shows that the wrinkling mode is localised near the inner rim due to the stress concentration and the small bending stiffness of the plate, then how will the discontinuity of the bi-annular plate affect the wrinkling mode? Is it possible that the wrinkling is still triggered near the inner boundary or the interface, or that we have two localised wrinkles on both annuli?

Moreover, the critical wrinkling load increases monotonically with the aspect ratio (ratio between the inner and outer radii of the single annulus), so is the critical wrinkle number for the simple annular plate. Whereas, for the stretched bi-annular plate, we find that the relations are not continuous as the former, or it might not be monotonic in some cases.

Also, in the compressed situations discussed by Simitses and Frostig, the authors discussed mainly the buckling forces of either when the mode number $n = 0$ (axisymmetric mode) or $n = 1$ (asymmetric mode). However, the wrinkling mode number in our problem is supposed to be $n \gg 1$, similar with the localised wrinkling problem in [4], [5]. In this case, the critical wrinkling mode number becomes a pivotal extra parameter for the critical wrinkling loads; Moreover, their models (compressive ones) are only subjected to uniformly compressive stresses, therefore, the buckling is *global*, the mechanical properties of both annuli all make contribution to the *global* buckling. In other words, there is no dominant effect introduced by the mechanical parameters of either sub-annular region. While in the present problem, the buckling is expected to be localised in the case of the stretched single annular plate, it is interesting to see if only the mechanical properties of the localised region plays the dominant role compared with the flatter region.

To answer the above questions, we organise the paper as follows. In Section II, we introduce the problem and record the formulation for the wrinkling of a bi-annular plate. The For thin plates, the analysis of the pre-buckling always can provide fruitful indication for the wrinkling load, which is expanded in Section III. With this in mind, we conduct extensive numerical explorations. The critical wrinkling load and the corresponding critical wrinkling modes are shown in Section IV. In these sections, we fully answered the questions raised earlier. The paper ends with a concluding section and some possible extensions that will be taken up in future work.

II. PROBLEM STATEMENT AND FORMULATION

Let us consider a simple plane-stress situation that generalises the Lamé problem for an annular domain subjected to radial stresses or displacements on its inner and outer boundaries.

Rather than having uniform elastic properties the annulus, Ω (say), is assumed to consists of two perfectly bonded concentric annular regions,

$$\Omega_I := \left\{ (r,\theta) \in \mathbb{R}^2 \mid R_1 \le r \le R_m, \quad 0 \le \theta < 2\pi \right\},$$

$$\Omega_{II} := \left\{ (r,\theta) \in \mathbb{R}^2 \mid R_m \le r \le R_2, \quad 0 \le \theta < 2\pi \right\},$$

that have different mechanical properties, i.e. $\Omega = \Omega_I \cup \Omega_{II}$ (details of the geometry that we have in mind can be seen in Figure 1). For the sake of simplicity it will be assumed that the thicknesses of the two annuli is identical and equal to $h > 0$. The inner and outer rims of Ω are given by the curves $r = R_1$ and $r = R_2$, respectively, while $r = R_m$ indicates the location of the interface between the two concentric regions. The inner annulus (Ω_I) consists of a linearly elastic isotropic material characterised by the Young's modulus E_1 and Poisson's ratio ν_1; the outer region (Ω_{II}) is similar, but its material is described by the elastic constants E_2 and ν_2. In addition, the inner and outer rims are assumed to subjected to displacement field U_1 (inward) and U_2 (outward) respectively.
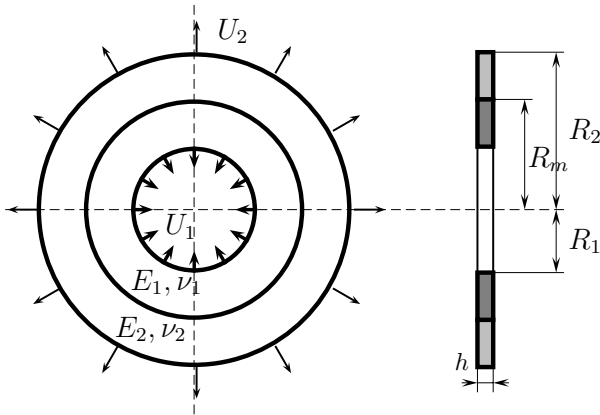

Fig. 1. A bi-annular plate stretched by applied uniform displacements on both its inner and outer edges. The two constituent parts Ω_I and Ω_{II} are assumed to be perfectly bonded together.

We take the vector $\boldsymbol{x} = \boldsymbol{y} + x_3 \boldsymbol{e}_3$ to describe the position of points within the plate, where $x_3 \in [-h/2, h/2]$ stands for the lateral coordinate (h is the thickness of the plate), and $\boldsymbol{y} = x_\alpha \boldsymbol{e}_\alpha \in \Omega$ denotes the two-dimensional components in the mid-plane surface, where $\alpha \in \{r,\theta\}$ as polar coordinates are applied. The in-plane displacement is defined as $\boldsymbol{v} := (u, v)$, and the lateral displacement is described by w.

For the notational convenience, we use the labels $j = I$ or II to indicate the variables in two regions: Ω_I and Ω_{II}, and use "∘" to denote the variables in basic state. By using principle of minimum energy [11], the equations governing the basic state for both annuli of the plate can be obtained [7], [13] as

$$\boldsymbol{\nabla} \cdot \mathring{\boldsymbol{N}}^{(j)} \equiv 0 \quad \text{in} \quad \Omega_{(j)}, j \in \{I, II\}, \tag{1}$$

together with the natural interfacial conditions

$$\mathring{\boldsymbol{N}}^I \equiv \mathring{\boldsymbol{N}}^{II} \quad \text{on} \quad r = R_m. \tag{2}$$

In addition, the forced boundary conditions are prescribed as

$$\mathring{\boldsymbol{v}}^I = (-U_1, 0) \text{ on } r = R_1, \quad \mathring{\boldsymbol{v}}^{II} = (U_2, 0) \text{ on } r = R_2. \tag{3}$$

Here, we introduce the non-dimensional variables

$$\rho := \frac{r}{R_2}, \quad \eta_1 := \frac{R_1}{R_2}, \quad \eta_2 := \frac{R_m}{R_2}, \quad \lambda := \frac{U_1}{U_2},$$

$$\gamma := \frac{E_1}{E_2}, \quad \mathring{\sigma}_{kk} \to \frac{1 - \nu_{(j)}^2}{E_{(j)}} \mathring{\sigma}_{kk}, \quad k \in \{r, \theta\}, \; j \in \{I, II\}.$$

If we assume axial symmetry, then (1) together with (2) and (3) will lead to the classical Lamé solution in terms of the stress components in both radial and azimuthal directions (under the assumption that the thickness of the whole plate is unique)

$$\begin{bmatrix} \mathring{\sigma}_{rr}^{(j)} \\ \mathring{\sigma}_{\theta\theta}^{(j)} \end{bmatrix} \to \begin{bmatrix} 1 + \nu_{(j)} & -\dfrac{1 - \nu_{(j)}}{\rho^2} \\ 1 + \nu_{(j)} & \dfrac{1 - \nu_{(j)}}{\rho^2} \end{bmatrix} \begin{bmatrix} b^{(j)} \\ c^{(j)} \end{bmatrix}, \qquad j \in \{I, II\}. \tag{4}$$

with the coefficients

$$b^{(j)} = \frac{1}{\Delta}(\Gamma_{11}^{(j)}\lambda + \Gamma_{12}^{(j)}), \quad c^{(j)} = \frac{1}{\Delta}(\Gamma_{21}^{(j)}\lambda + \Gamma_{22}^{(j)}), \tag{5}$$

and where

$$\Gamma_{11}^I := \left[(\kappa_3 + \kappa_2)\eta_2^2 + (\kappa_4 - \kappa_2) \right] \eta_1,$$
$$\Gamma_{12}^I := (\kappa_3 + \kappa_4)\eta_2^2,$$
$$\Gamma_{21}^I := -\left[(\kappa_3 - \kappa_1)\eta_2^2 + (\kappa_1 + \kappa_4) \right] \eta_1\eta_2^2,$$
$$\Gamma_{22}^I := -(\kappa_3 + \kappa_4)\eta_1^2\eta_2^2,$$
$$\Gamma_{11}^{II} := (\kappa_1 + \kappa_2)\eta_1\eta_2^2,$$
$$\Gamma_{12}^{II} := (\kappa_1 + \kappa_4)\eta_2^2 + (\kappa_2 - \kappa_4)\eta_1^2,$$
$$\Gamma_{21}^{II} := -(\kappa_1 + \kappa_2)\eta_1\eta_2^2,$$
$$\Gamma_{22}^{II} := -\left[(\kappa_2 + \kappa_3)\eta_1^2 + (\kappa_1 - \kappa_3)\eta_2^2 \right].$$

with

$$\kappa_1 := \frac{\gamma}{1 - \nu_1}, \quad \kappa_2 := \frac{\gamma}{1 + \nu_1}, \quad \kappa_3 := \frac{1}{1 - \nu_2}, \quad \kappa_4 := \frac{1}{1 + \nu_2}.$$

$$\Delta := \left[\kappa_2 - \kappa_4 - (\kappa_3 + \kappa_2)\eta_2^2 \right]\eta_1^2 + \left[(\kappa_3 - \kappa_1)\eta_2^2 + \kappa_1 + \kappa_4 \right]\eta_2^2.$$

According to the Trefftz criterion (see for example, [11]), the perturbation equations for the wrinkling state is given [13] by

$$D_{(j)}\nabla^4 w^{(j)} - \mathring{\boldsymbol{N}}^{(j)} : (\boldsymbol{\nabla} \otimes \boldsymbol{\nabla} w^{(j)}) = 0 \quad \text{in} \quad \Omega_{(j)}, \tag{6}$$

which is applicable to the inner and outer sub-annular regions by taking $j = I$ and II respectively. If we introduce the following rescaling

$$w^{(j)} \to \frac{w^{(j)}}{h}, \qquad D_{(j)} \to \frac{h^2}{12U_2R_2} =: \mu^{-2}, \tag{7}$$

We can write the rescaled versions of (6) in the compact form

$$\mu^{-2}\nabla^4 w^{(j)} - h\left[\mathring{\sigma}_{rr}^{(j)} \frac{\partial^2 w^{(j)}}{\partial\rho^2} + \mathring{\sigma}_{\theta\theta}^{(j)} \frac{1}{\rho}\left(\frac{\partial w^{(j)}}{\partial\rho} \right.\right.$$
$$\left.\left. + \frac{1}{\rho}\frac{\partial^2 w^{(j)}}{\partial\theta^2} \right) \right] = 0, \tag{8}$$

where μ^{-2} is usually a very small parameter ($0 < \mu^{-1} \ll 1$) for plates that are very thin or highly stretched (within the limits of the theory employed in our investigations). By looking for solutions with separable variables we are prompted to consider

$$w^{(j)}(\rho, \theta) = W^{(j)}(\rho) \cos(n\theta), \quad j \in \{I, II\}, \qquad (9)$$

where $n \in \mathbb{N}$ represents the mode number (equal to half the number of regular wrinkles in the azimuthal direction), and the unknown amplitudes $W^{I,II}$ will be found by solving the following simpler ordinary differential equations

$$\frac{d^4 W^{(j)}}{d\rho^4} + \mathcal{C}_3^{(j)}(\rho)\frac{d^3 W^{(j)}}{d\rho^3} + \mathcal{C}_2^{(j)}(\rho)\frac{d^2 W^{(j)}}{d\rho^2}$$
$$+ \mathcal{C}_1^{(j)}(\rho)\frac{dW^{(j)}}{d\rho} + \mathcal{C}_0^{(j)}(\rho)W^{(j)} = 0, \quad \rho \in \Lambda_{(j)} \quad (10)$$

in which

$$\mathcal{C}_3^{(j)}(\rho) := \frac{2}{\rho},$$
$$\mathcal{C}_2^{(j)}(\rho) := -\left[\frac{2n^2 + 1}{\rho^2} + \mu^2\,\mathring{\sigma}_{\rho\rho}^{(j)}(\rho)\right],$$
$$\mathcal{C}_1^{(j)}(\rho) := \frac{1}{\rho}\left[\frac{2n^2 + 1}{\rho^2} - \mu^2\,\mathring{\sigma}_{\theta\theta}^{(j)}(\rho)\right],$$
$$\mathcal{C}_0^{(j)}(\rho) := \frac{n^2}{\rho^2}\left[\frac{n^2 - 4}{\rho^2} + \mu^2\,\mathring{\sigma}_{\theta\theta}^{(j)}(\rho)\right].$$

and where $j = I$ or II is adopted, respectively, to describe the buckling equations of the inner and outer sub-regions. the kinematic continuity on the interface requires that

$$w^I = w^{II}, \quad \nabla_r w^I = \nabla_r w^{II} \quad \text{at} \quad r = R_m \qquad (11)$$

due to the axisymmetry of the problem. We have the continuity constraint on $r = R_m$

$$-D_I\left[\nabla_r(\nabla^2 w^I) + (1 - \nu_1)\nabla_\theta(\nabla_{r\theta} w^I)\right]$$
$$= -D_{II}\left[\nabla_r(\nabla^2 w^{II}) + (1 - \nu_2)\nabla_\theta(\nabla_{r\theta} w^{II})\right], \quad (12)$$

which is the equilibrium of the vertical shear force resultants on the interface written on the deformed configuration.

$$D_I(\nabla_{rr}w^I + \nu_1 \nabla_{\theta\theta}w^I) = D_{II}(\nabla_{rr}w^{II} + \nu_2 \nabla_{\theta\theta}w^{II}), \quad (13)$$

which states the equilibrium of the bending moments on interface. These conditions can be rescaled easily by using the previously introduced rescalings.

III. BASIC STATE

Next, we are going to study the existence of azimuthal compressive stresses in Ω as in Eq. (4). Since for thin (slender) structures, the analysis on the compressive stress in the basic state can always provide fruitful predictions on the buckling problem. However, for a stretched bi-annular plate, the azimuthal stresses are complicated compared with the single-annular case in [4], [5], therefore demand some analysis. For the sake of notational convenience, we denote

the pre-buckling hoop stress on the boundaries and interface by

$$I_a := \sigma_{\theta\theta}^{(0)I}(\eta_1), \quad I_b := \sigma_{\theta\theta}^{(0)I}(\eta_2), \qquad (14a)$$
$$II_a := \sigma_{\theta\theta}^{(0)II}(\eta_2), \quad II_b := \sigma_{\theta\theta}^{(0)II}(1). \qquad (14b)$$

It is interesting to notice that $I_a < I_b$ and $II_a < II_b$ for all the situations, which requires some standard numerical exploring. The main task of prebuckling stresses analysis is to identify the lower bound for the value of λ when I_a or II_a firstly changes from positive to negative, which motivates the analytical investigations included next.

If we let $I_a(\eta_1, \eta_2; \lambda) = 0$, then with fixed η_2, it can be shown that

$$\lambda_1^{\text{low}} = \frac{l_1 \eta_1}{l_2 \eta_1^2 + l_3 \eta_2^2}, \qquad (15)$$

by introducing

$$l_1 := \frac{4\gamma\nu_1\eta_2^2}{(1 - \nu_1^2)(1 - \nu_2^2)}, \quad l_2 := \kappa\left[\kappa_2(1 - \eta_2^2) - (\kappa_4 + \kappa_3\eta_2^2)\right],$$
$$l_3 := \kappa_2\left[\kappa_1(1 - \eta_2^2) + (\kappa_4 + \kappa_3\eta_2^2)\right].$$

Some fundamental analysis reveals that λ_1^{low} is zero when $\eta_1 = 0$, and it increases monotonically (always positive) before the denominator of the above expression changes sign from positive to negative. More specifically, $\lambda_1^{\text{low}} \to \infty$ at

$$\eta_1 = \eta_2\sqrt{\frac{(1 - \nu_2)l_3 + (1 + \nu_2)l_4\eta_2^2}{(1 - \nu_2)l_5 + (1 + \nu_2)l_6\eta_2^2}},$$

where

$$l_3 := 1 - \nu_1 + \gamma(1 + \nu_2), \quad l_2 := 1 - \nu_4 - \gamma(1 - \nu_2),$$
$$l_5 := 1 + \nu_1 - \gamma(1 + \nu_2), \quad l_6 := 1 + \nu_1 + \gamma(1 - \nu_2).$$

provided the coefficient of η_2 above falls between 0 and 1, namely

$$\eta_2 > \sqrt{\left(\frac{1 - \nu_2}{1 + \nu_2}\right) \cdot \frac{\gamma(1 + \nu_2) - \nu_1}{\gamma(1 + \nu_2) + \nu_1}} := \bar{\eta}_2.$$

Similarly, if we let $I_a(\eta_1, \eta_2; \lambda) = 0$, we have

$$\lambda_2^{\text{low}} = l_7\left(l_8\frac{\eta_2^2}{\eta_1} - l_9\eta_1\right), \qquad (16)$$

where

$$l_7 := \left(\frac{1 - \nu_1^2}{1 - \nu_2^2}\right) \cdot \frac{1}{\gamma\left[1 - \nu_2 - (1 + \nu_2)\eta_2^2\right]},$$
$$l_8 := (1 + \nu_1)(1 - \nu_1 + \gamma\nu_2), \quad l_9 := (1 - \nu_1)(1 + \nu_1 - \gamma\nu_2).$$

Actually, λ_2^{low} can be easily proved to be a monotonically decreasing function of η_1. It can be pointed out there are two types of such lower bound for λ^{low}: one is of monotonic shape only presents to be λ_1^{low}; the other is of kink shape which is the conjunction of λ_1^{low} and λ_1^{low}. In the latter case, the "kink" can be understood mathematically as the point where $I_a = II_a = 0$ when $\eta_1 > 0$ and $\lambda > 0$. Solving $\lambda_1^{\text{low}}(\eta_1) = \lambda_2^{\text{low}}(\eta_1)$ and dropping the invalid roots of η_1, we are left with the root

$$\eta_1^{\text{kink}} = \eta_2\sqrt{\frac{1 - \nu_1 + \gamma\nu_2}{1 + \nu_1 - \gamma\nu_2}};$$

thus, the possibility of the "kink" is guaranteed by forcing the intersecting point η_1^{kink} to be within $(0, \eta_2)$, which requires $0 < \gamma < \nu_1/\nu_2$. On the contrary, once $\gamma > \nu_1/\nu_2$, then η_1^{kink} falls outside $(0, \eta_2)$, therefore, $\lambda^{\text{low}}(\eta_1)$ appears to be monotonic-shape. In conclusion,

$$0 < \gamma < \nu_1/\nu_2, \qquad \text{kink shape } \lambda^{\text{low}}, \tag{17a}$$

$$\gamma > \nu_1/\nu_2, \qquad \text{monotonic shape } \lambda^{\text{low}}. \tag{17b}$$

IV. RESULTS FOR WRINKLING PROBLEM

A. Neutral stability curve

Now we are in position to investigate the role played by the mechanical parameters γ, ν_1 and ν_2 on the neutral stability (characterised by parameters λ_C, n_C) of the stretched annular plate, where, $\lambda_C(\eta_1) = \min_{n \in \mathbb{N}} \lambda(\eta_1)$ is the critical wrinkling load, and n_C is the corresponding critical wrinkling mode number. We fix the interface location η_2 and the large parameter μ ($\mu \ll 1$) and solve the eigenproblem numerically [1]–[3], [12], [15] by using an optimal strategy.

Firstly, we found that higher elasticity modulus ratio $\gamma := E_1/E_2$ will reduce the resistance of the wrinkling of a stretched bi-annular plate. Fig. 2 illustrates a range values of $\gamma = 0.5, 1$ and 2 all with fixed Poisson ratio $\nu_1 = \nu_2 = 0.3$ and $\eta_2 = 0.5$. It is easily seen that the three curves range in sequence with different γ for all range of η_1. It means that with Poisson ratios fixed, the smaller γ is, the larger λ_C will be, which is valid for the all range of $\eta_1 \in (0, \eta_2)$; as $\eta_1 \to \eta_2$, whatever the value of γ is, all the curves of λ_C coincide at a limit point (same for n_C). At this point, the inner annulus disappears, the bi-annular shrinks to a single annulus with inner radius η_2 and Poisson ratio ν_2, which is the same as the single-annular case in [4], [5]. We have also conducted systematical numerical simulations on various combinations of Poisson ratio of this two annuli, which verify the above conclusions.

Secondly, as γ fixed it is found that ν_1 plays a dominant role on the the neutral stability (λ_C, n_C) when η_1 is away from η_2, while as $\eta_1 \to \eta_2$, ν_2 appears to be of controlling effect. Fig. 3 shows the effect of Poisson ratios of the two annuli on the tensile instability of bi-annular plate with fixed $\gamma = 1$. It is interesting to notice that in Fig. 3(a), the *yellow dots* ($\nu_1 = 0.3, \nu_2 = 0.1$) follows immediately the *red continuous line* ($\nu_1 = \nu_2 = 0.3$) when $\eta_1 < 0.4$ or so. Also, the curves of *black circles* ($\nu_1 = 0.1, \nu_2 = 0.3$) and its counterpart *blue continuous line* ($\nu_1 = \nu_2 = 0.1$) approaches each other when $\eta_1 < 0.4$. This feature also applies for the corresponding curves in Fig. 3(b) for the n_C. Moreover, we found that with fixed γ, both the curves of λ_C and n_C approach its limit points when $\eta_1 \to \eta_2$ as ν_2 is the same (the *red continuous line* and *black circles*, the *blue continuous line* and the *yellow dots*), which matches closely with the earlier conclusions. Interestingly enough, our extensive numerical simulations suggest two representative types of neutral stability curves for λ_C, namely, the "kink" type (*yellow dots* in Fig. 2 and 3) and the "monotonic" type (*black circles* therein), which are both different from the curves of stretched single-annular plate(*continuous lines*). For the "kink" type neutral stability
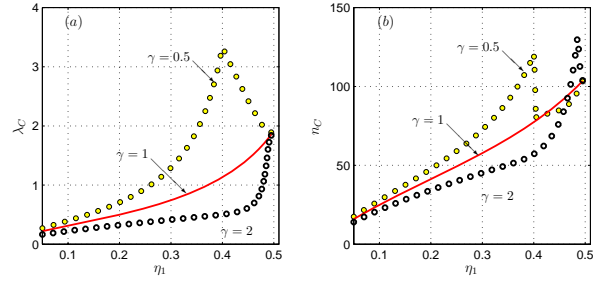

Fig. 2. Dependence of the critical eigenvalues λ_C and the corresponding critical mode number on the ratio of Young's modulus of two annuli $\gamma := E_1/E_2$, other parameters are: $\nu = 400, \nu_1 = \nu_2 = 0.3, \eta_2 = 0.5$.
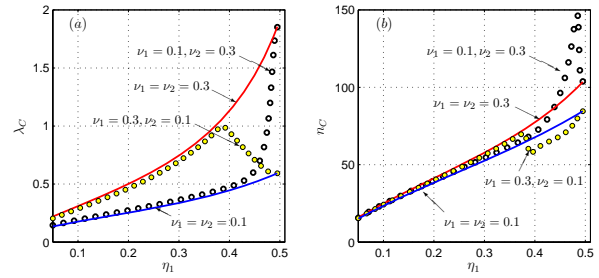

Fig. 3. Dependence of the critical eigenvalues λ_C and the corresponding critical mode number on the Poisson ratio of two annuli ν_1, ν_2; the other parameters are taken as $\nu = 400, \gamma := E_1/E_2 = 1, \eta_2 = 0.5$.

curves, with the increasing η_1, λ_C increases first up to the "kink", then descends monotonically until η_1 approaches η_2. While, in the "monotonic" type curves, λ_C increases with η_1 monotonically.

B. Critical wrinkling modes and morphological changes

Both the "monotonic" and "kink" features can be traced back to the pre-buckling hoop stress analysis in Section III, which is the case for $\mu \to \infty$. For the plate scenario ($0 < \mu < \infty$) that information is not immediately relevant, although
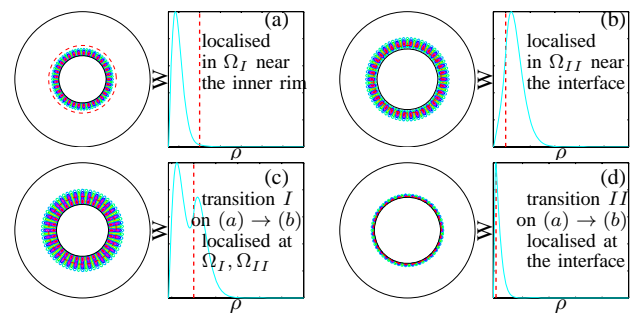

Fig. 4. Four types of wrinkling patterns.

for very large values of μ, we expect the latter situation to mirror closely the former. Therefore, we will try to understand by means of the pre-buckling analysis and the corresponding critical eigenmodes.

(1) "kink" type neutral stability curves are incident to the stretched bi-annular plate with flexible inner annulus (as indicated in basic state analysis, $0 < \gamma < \nu_1/\nu_2$), which follows the features of the lower bound λ^{low} as discussed in Section III. When η_1 is on the left but not close to the "kink", the critical eigenmodes are within region Ω_I and localised to its inner rim $\rho = \eta_1$ (Fig. 4(a)). Also, on the right side of the "kink", when $\eta_1 \to \eta_2$, the critical eigenmodes are localised to the interface within region Ω_{II}(Fig. 4(b)), which approaches the limiting case of the stretched single-annular plate with η_2 as its inner rim. However, there is an interesting transition between the aforementioned two types of eigenmodes, coinciding with the vicinity of the "kink" of kink shape λ_C curve. With the largest amplitude normalisation to 1, the localised part in Ω_I shrink gradually as η_1 approaches the "kink", meanwhile, there is a bump increase in Ω_{II} near the interface. When η_1 nearly approaches the "kink", the amplitudes of the wrinkles in both regions are not neglectalbe (Fig. 4(c)). Note that this is also when n_C shifts from its maximum, which means that at this stage, the wrinkled bi-annular plate displays the maximum number of wrinkles and these are localised in both regions near the interface. On passing this point, the bump in Ω_{II} enlarges with the decrease of that in Ω_I, at the same time, λ_C decreases and n_C shifts from its maximum to a smaller value where discontinuity occurs.

(2) As indicated from the pre-buckling hoop stress analysis in Section III, a stretched bi-annular plate with flexible inner annulus tend to have"monotonic" type neutral stability curves. However, it must be noticed that this type is different from the monotonic ones of stretched single-annular plate in two points: On the one hand, λ_C is very small when η_1 is not near η_2, then increases sharply as η_1 approaches η_2, displaying a blow-up like trend before arrives to it limit as η_1 superposes with η_2. On the other hand, the plots of n_C are not monotonic increasing with respect to η_1, but start at a small value then jump to its maximum when η_1 is near η_2, then return to a limit value at $\eta_1 = \eta_2$.

These significant features can be understood further by looking at the critical eigenmodes. The critical eigenmodes when η_1 is far away from η_2 or when $\eta_1 \to \eta_2$ are localised in Ω_I (Fig. 4(a)) and Ω_{II} (Fig. 4(b)) respectively, just similar with the case in kink λ_C curves. However, this monotonic-type λ_C has other features for the transition point (Fig. 4(d)): on the process of η_1 going close to η_2, the localised wrinkles move towards the interface, until it starts to cross the interface as λ_C increase sharply; when the wrinkle crest crosses the interface, n_C reaches its first local maximum; after that, the critical mode shift to the mode localised in Ω_{II} as soon as n_C drop rapidly to its limit point at η_2. It is to be emphasised that during the whole range of η_1, there is only one bump for the critical mode, distinct from that of the former "kink" type. From a physical point of view, the transition of the critical eigenmodes occurs when the critical wrinkle number is in the vicinity of its maximum. Also, this occurence happens as the two-bump wrinkles or the wrinkle crest passes the interface, which requires much higher elastic energy to buckle, thus, for $\mu \gg 1$ such a case is only noticeable for an extremely narrow window of $0 < \eta_1 < \eta_2 < 1$. Furthermore, because the Young's modulus E_2 has been rescaled out, when $\gamma := E_1/E_2$ is fixed, the Poisson ratio of the localised region plays a dominant role on the critical external loading λ_C.

V. Conclusion

The problem of tensile wrinkling for a radially stretched thin annular plate [5] has been extended to a system consisting of two (mechanically different) concentric annular plates perfectly bounded along a circular interface. The wrinkling problem is predicted firstly by the analysis of basic state for a limit case as $\mu \to \infty$, the analysis also provides a two types of neutral stability curves, the so called kink-type and monotonic-type, which correspond to the conditions of the relations of parameters whether $\gamma := E_1/E_2$ is smaller or larger than ν_1/ν_2. Extensive numerical simulations have been carried out by using numerical strategies of an adapted version of compound matrix method, in conjugation with a advanced collocation solver $sbvp$. The response curves and neutral stability curves are obtained with respect to different combinations of the mechanical parameters of the two annuli. The neutral stability curves also can be classified into two different types, the *monotonic* and the *kink* shape. More specifically, a bi-annular plate with more flexible inner part $E_1/E_2 < \nu_1/\nu_2$ is typically seen a "kink" shape neutral stability curves, and of higher resistance against wrinkling under stretching (defined by $\lambda = U_1/U_2$), while such a plate with stiffer inner annulus is tend to appear a "monotonic" shape neutral stability curves with lower critical external stretching. By further investigations on the critical eigenmodes, we have gained a deeper understanding on the effects of the discontinuities of the interface on either the critical external stretching and the wrinkling mode. The strategy presented in this paper can be extended to more number of concentric annuli that make up the multi-annular plate. It would be of interest to know how the kink-like feature in the critical stability envelope is modified by the addition of at least another annular sub-region, how the discontinuities affect the wrinkling patterns. Also, the singular-perturbed feature of this problem enable use to conduct asymptotic analysis, and this is the subject of a forthcoming work [6].

REFERENCES

[1] U. Ascher and R. D. Russell. Reformulation of Boundary Value Problems into "Standard" Form. *SIAM Review*, 23(2):238–254, 1981.

[2] Winfried Auzinger, Gnter Kneisl, Othmar Koch, and Ewa Weinmller. Sbvp 1.0 - a matlab solver for singular boundary value problems. Technical report, Institute for Applied Mathematics and Numerical Analysis, http://www.math.tuwien.ac.at/ ewa/, 2002.

[3] Winfried Auzinger, Gnter Kneisl, Othmar Koch, and Ewa Weinmller. A collocation code for singular boundary value problems in ordinary differential equations. *Numerical Algorithms*, 33:27–39, 2003. 10.1023/A:1025531130904.

[4] C.D. Coman and A.P. Bassom. On the wrinkling of a pre-stressed annular thin film in tension. *Journal of the Mechanics and Physics of Solids*, 55:1601–1617, 2007.

[5] C.D. Coman and D.M. Haughton. Localised wrinkling instabilities in radially stretched annular thin films. *Acta Mech.*, 185:179–200, 2006.

[6] C.D. Coman and X. Liu. Buckling-resistant thin annular plates in tension. 2012. (submitted for publications 2012).

[7] C.D. Coman and X. Liu. Semi-analytical approximations for a class of multi-parameter eigenvalue problems related to tensile buckling. *Z. angew. Math. Phys.*, 2012. (accepted, May 2012).

[8] Y Frostig and GJ Simitses. Buckling of multi-annular plates. *Computers & Structures*, 24(3):443–454, 1986.

[9] Y Frostig and GJ Simitses. Buckling of ring-stiffened multi-annular plates. *Computers & Structures*, 29(3):519–526, 1988.

[10] J. C. Géminard, R. Bernal, and F. Melo. Wrinkle formations in axis-symmetrically stretched membranes. *The European Physical Journal E*, 15:117–126, 2004.

[11] Henry Louis Langhaar. *Energy methods in applied mechanics*. Wiley, 1962.

[12] K. A Lindsay. The application of compound matrices to convection problems in multi-layered continua. *Mathematical Models and Methods in Applied Sciences*, 2(2):121–141, 1992.

[13] X. Liu. *On some eigenvalue problems for elastic instabilities in tension*. PhD thesis, University of Glasgow, 2012.

[14] GJ Simitses. Effect of boundary conditions and rigidities on the buckling of annular plates. *Thin-Walled Structures*, 5, 1987.

[15] O. Koch W. Auzinger, E. Karner and E. Weinmüller. Collocation methods for the solution of eigenvalue problems for singular ordinary differential equations. *Opuscula Math.*, 26(2):pp. 229–241, 2006.